Aerosol and Air Quality Research, 18: 1294–1304, 2018

ISSN: 1680-8584 print / 2071-1409 online
doi: 10.4209/aaqr.2017.12.0603

Source Apportionment and Risk Assessment of Atmospheric Polycyclic Aromatic Hydrocarbons in Lhasa, Tibet, China

Pengfei Chen[1], Shichang Kang[1,2*], Chaoliu Li[2,3], Quanlian Li[1], Fangping Yan[4], Junming Guo[1], Zhenming Ji[3], Qianggong Zhang[2,3], Zhaofu Hu[1], Lekhendra Tripathee[1], Mika Sillanpää[4,5]

[1] *State Key Laboratory of Cryospheric Science, Northwest Institute of Eco-Environment and Resources, Chinese Academy of Sciences (CAS), Lanzhou 730000, China*
[2] *CAS Center for Excellence in Tibetan Plateau Earth Sciences, Beijing 100085, China*
[3] *Key Laboratory of Tibetan Environment Changes and Land Surface Processes, Institute of Tibetan Plateau Research, CAS, Beijing 100101, China*
[4] *Laboratory of Green Chemistry, Lappeenranta University of Technology, 50130 Mikkeli, Finland*
[5] *Department of Civil and Environmental Engineering, Florida International University, Miami, FL-33174, USA*

ABSTRACT

Much attention has been given to the distributions, sources, and health risks of atmospheric polycyclic aromatic hydrocarbons (PAHs) in cities. In this study, a total of 62 suspended particle samples were collected from April 2013 till March 2014 in the city of Lhasa. Positive matrix factorization (PMF) was applied to investigate the source apportionment of 15 priority PAHs, the lifetime carcinogenic risk (LCR) levels of which were assessed. The average annual particle phase PAH concentration was 43.9 ± 60.4 ng m^{-3}. Evident seasonal variations of PAHs were observed, with the highest concentration observed in winter, followed by autumn, spring, and summer. Four- and five-ring PAHs accounted for the predominant proportion (63.3%–84.4%) throughout the year. Correspondingly, gas phase PAHs showed the opposite variations, with the highest and lowest concentrations observed in summer and winter, respectively; also, three-ring PAHs, especially Ace, Acel, and Flu, were the largest contributors. Compositions of particle phase PAHs varied seasonally, with four-ring PAHs contributing more in winter than in summer and five-ring PAHs exhibiting the opposite trend, thereby reflecting the variety of emission sources. PMF analysis showed that biomass combustion (48.4%) and vehicle emissions (27.9%) were the two main sources, followed by coal combustion and the air–surface exchange. These results were consistent with the diagnostic molecular ratios. The benzo(a)pyrene equivalent (BaP_{eq}) concentration of particle phase PAHs ranged from 1.48 to 24.5 ng m^{-3}, which exceeds were higher than the new limit in China (1 ng m^{-3}). The average BaP_{eq} of gas phase PAHs was 6.43 ± 4.15 ng m^{-3}, which was similar to that of particle phase PAHs. The LCR of the total PAHs (9.08×10^{-6}) was one time higher than that of the particle phase; however, it was slightly lower than the acceptable level, thereby indicating that atmospheric PAHs in Lhasa pose little or no carcinogenic risk to the local population.

Keywords: Polycyclic aromatic hydrocarbons; Source apportionment; Health risk; Tibetan Plateau.

INTRODUCTION

Polycyclic aromatic hydrocarbons (PAHs) compose a large group of organic compounds that consist of fused aromatic rings. They are emitted mainly from the incomplete combustion or pyrolysis of organic materials such as coal, oil, gas, waste, and biomass (Ravindra *et al.*, 2008; Zhang and Tao, 2009). PAHs are the subject of considerable concern because of their potential risk to the environment and human health (Bhargava *et al.*, 2004; Lai *et al.*, 2017; Liu *et al.*, 2017a; Saha *et al.*, 2017; Yang *et al.*, 2017). As persistent semivolatile chemicals, PAHs can be transported over long distances to remote areas such as polar regions (Halsall *et al.*, 2001; Huang *et al.*, 2005) and high altitude regions such as the Tibetan Plateau (TP) (Wang *et al.*, 2014; Chen *et al.*, 2017).

The TP is one of the world's least scientifically studied regions in terms of PAH concentration, composition, transportation, source apportionment, and health risk assessment. Anthropogenic emissions within the TP are not of major concern compared with those in densely populated and industrialized parts of South and East Asia. Traditional agriculture and animal husbandry are the main

*Corresponding author.
Tel: +86-0931-4967368; Fax: +86-0931-4967368
E-mail address: shichang.kang@lzb.ac.cn;
chenpengfeifeifei@126.com

economic pillars of the TP, whereas industry accounts for only 8% of the gross domestic product of this region (http://www.tibet.stats.gov.cn/). Therefore, the TP is considered a background site on a global scale. Numerous recent studies have reported atmospheric pollutants in this remote region (Cong *et al.*, 2015a; Lüthi *et al.*, 2015; Li *et al.*, 2016); however, such studies have primarily been concerned with the role of the long-range transportation of pollutants emitted from South Asia. Notably, local anthropogenic activity in the TP contributes significantly to the atmospheric environment (Gong *et al.*, 2011; Li *et al.*, 2012; Chen *et al.*, 2015a; Li *et al.*, 2016a).

Lhasa, the provincial capital of Tibet, is currently undergoing rapid urbanization and industrialization (Li and Wang, 2014; Ran *et al.*, 2014; Li *et al.*, 2016b). Previous studies have reported that the atmosphere in this high altitude city has been heavily influenced by local emissions (Huang *et al.*, 2010; Cong *et al.*, 2011; Li *et al.*, 2016b). In addition, as the largest city in the TP, emissions from Lhasa are potential pollution sources to the surrounding areas (Li *et al.*, 2008; Tao *et al.*, 2010); for example, higher elemental and organochlorine pesticide concentrations were reported in aerosol samples from Lhasa than in those from more remote sites in the TP (Li *et al.*, 2008; Cong *et al.*, 2011). Current use and local emissions of organochlorine pesticides may contribute to environmental contamination in the populated agricultural Lhasa River Basin (Li *et al.*, 2008). Radiocarbon isotope measurements of total carbon emissions revealed biomass burning and the incineration of agricultural waste, which contributed more to carbonaceous aerosols in winter than summer (Huang *et al.*, 2010). Fine particulate matter ($PM_{2.5}$) in Lhasa is characterized by its low organic carbon to elemental carbon ratio, which reflects the heavy influence of vehicle emissions (Li *et al.*, 2016b). Regarding PAHs, two studies have reported atmospheric PAH concentrations and compositions in Lhasa (Gong *et al.*, 2011; Liu *et al.*, 2013). Diagnostic ratios and principal component analysis revealed that atmospheric PAHs in Lhasa were primarily derived from local human activities such as vehicle emissions and incense burning. However, current knowledge of PAH source apportionment and its effects on the health of locals in Lhasa remains limited.

This paper presents the results of particulate-phase PAH observations in Lhasa during 2013 to 2014. The main objectives were as follows: (1) to investigate the atmospheric PAH concentrations and compositions in Lhasa; (2) to identify the seasonal variations of PAH concentrations and apportion the PAH sources by using a positive matrix factorization (PMF) model; and (3) to assess the health risks experienced due to PAHs in Lhasa.

METHODS

Sample Collection

A total suspended particle (TSP) filter sampler (flow rate: 100 L min^{-1}; KC-120H, Qingdao Laoshan Applied Technology Institute, Qingdao, China) was placed on the rooftop (20 m above ground) of the Institute of Tibetan Plateau Research, Lhasa (E29.65°, N91.03°, 3642 m). A total of 62 samples were collected on prebaked quartz fiber filters (diameter: 90 mm; Whatman plc, Maidstone, United Kingdom) from April 2013 to March 2014 with duration of each sample as 24 h. TSP filter samples were collected continuously every week. For example, we collected 3 samples each week in spring but 1 sample in other seasons. However, several samples could not be collected due to lack of power or equipment breakdown in some periods. Finally, 19, 17, 11, and 15 samples were collected in spring, summer, autumn, and winter, respectively. All filters were prebaked at 550°C for 6 h before sampling. They were equilibrated at constant temperature and humidity (25 ± 3°C, 30 ± 5%) for 72 h and weighed using a microbalance with a sensitivity of ± 0.01 mg before and after sampling. The volume of air passing through each filter was converted into standard atmospheric conditions (25°C, 101.3 kPa). Ten field blank filters were collected once each month by placing in the sampler, which had no air drawn through it. And 3, 3, 2, and 2 blank filters were collected in spring, summer, autumn, and winter, respectively. Lhasa is a famous historic tourist city where considerable seasonal variations in traffic and religious activities occur. It exhibits the typical characteristics of four seasons, namely spring (March–May), summer (June–September), autumn (October–November), and winter (December–February). Meteorological parameters of studying period were recorded with automatic observation instruments at Lhasa Station. According to the observation, the air temperature ranged from –5.7 to 21.2°C with an average of 9.0°C, and the relative humidity ranged from 7 to 75% with an average of 38.7% (Wan *et al.*, 2016). The annual mean precipitation amount is around 400 mm with the majority of precipitation occurred frequently between June and September because of the summer monsoon activities, but it was relatively dry during spring and winter. The largest coal-fired power plant of Tibet (Dongga power plant) and the Dongga cement factory were located about 10 km west of our sampling site. In addition, our sampling site is close to Jinzhu Road which is one of the busiest roads in Lhasa city with large numbers of trucks and other vehicles running. These are potential sources of particles in the atmosphere (Huang *et al.*, 2013).

Extraction and Analysis

Sonication extraction was used as detailed in Chen *et al.* (2015b). Here, the method is described briefly. A quarter of each filter was cut into pieces, placed into a glass tube, and immersed in 20 mL of dichloromethane (DCM) and *n*-hexane (1:1). The extraction was performed by sonication twice at 27°C for 30 min. Every single sample was spiked with deuterated PAHs (naphthalene-d8, acenaphthene-d10, phenanthrene-d10, chrysene-d12, and perylene-d12) as recovery surrogates. The extracts were evaporated to about 0.5 mL with a rotary evaporator, and transferred to a multilayer column filled with 2 g of activated silica gel, 4 g of neutral alumina, and 1 cm of anhydrous Na_2SO_4 (pre-soaked in *n*-hexane). Then, the column was eluted by a mixture of 10 mL of *n*-hexane and 20 mL of DCM/*n*-hexane (1:1). The eluent solvent was blown down to a final volume of 1 mL under a gentle stream of nitrogen. Finally,

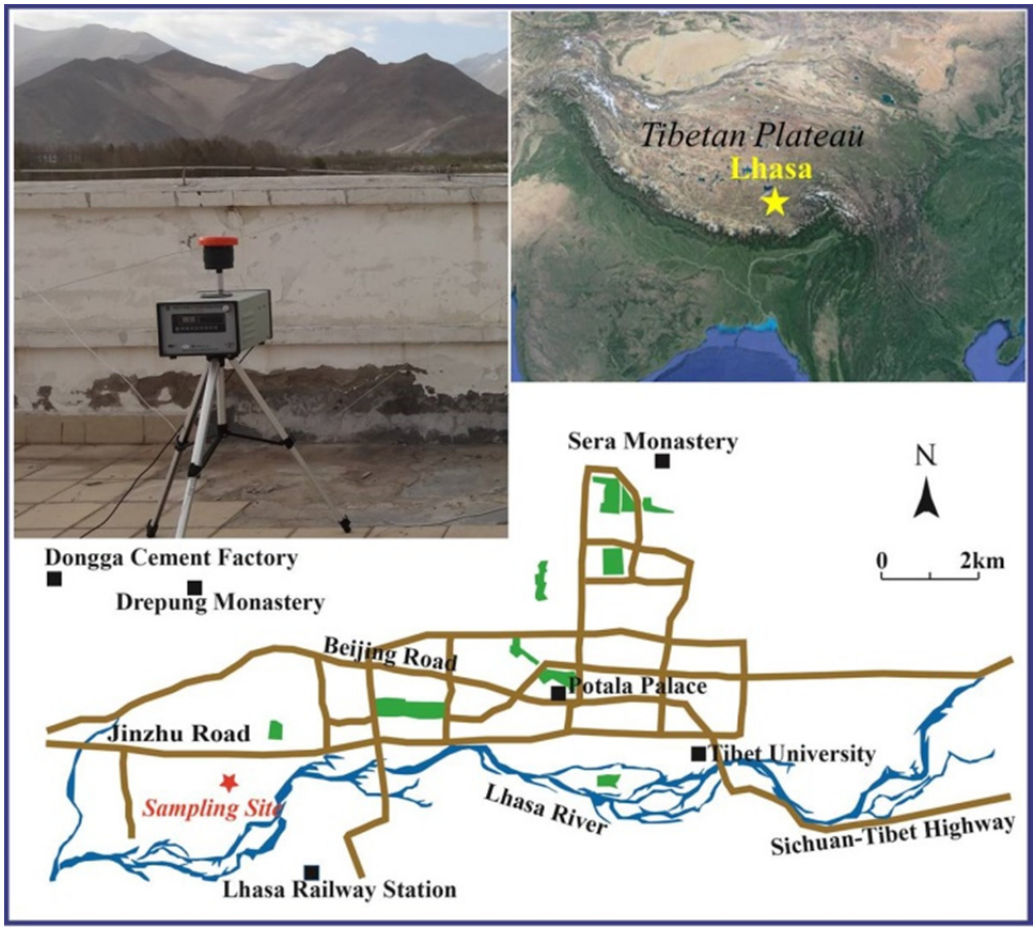

Fig. 1. Locations of sampling sites and the aerosol sampler (picture).

the solution was transferred to a 1.5-mL vial and stored at –20°C for rejection.

Sixteen PAHs (naphthalene (Nap), aecnaphthene (Ace), acenaphthylene (Aecl), anthracene (Ant), fluorene (Flu), phenanthrene (Phe), benzo(a)anthracene (BaA), chrysene (Chr), fluoranthene (Fla), pyrene (Pyr), benzo(a)pyrene (BaP), benzo(b)fluoranthene (BbF), benzo(k)fluoranthene (BkF), dibenzo(a,h)anthracene (DahA), benzo(g,h,i)perylene (BghiP) and indeno(1,2,3-cd)pyrene (IndP)) prioritized by the United States Environmental Protection Agency (US EPA) were analyzed at the State Key Laboratory of Cryospheric Sciences, Chinese Academy of Sciences Northwest Institute of Eco-Environment and Resources, China, by using gas chromatography–mass spectrometry with a 30 × 250-μm ID HP-5MS. High-purity helium was used as a carrier gas at a constant flow rate of 1.0 mL min^{-1}. The mass spectrometer was operated in 70-Ev electron impact mode. The oven temperature was 100°C, which was held stable for 2 min. Then it was ramped to the final temperature of 260°C with different rate of increase; to 170°C at 25 °C min^{-1}, to 225°C at 8 °C min^{-1}, to 235°C at 0.7 °C min^{-1}, to 260°C at 25 °C min^{-1}, and finally held at 260°C for 2 min. The temperature of the injector was 250°C and that of the transfer line was 280°C (Chen *et al.*, 2017). Nap was not analyzed as it was detected with high concentration in the laboratory and field blanks.

Quality Control

All analytic procedures were carried out using same method with strict quality assurance and control measures with Chen *et al.* (2017). Laboratory and field blanks were extracted and analyzed in the same way as the samples. The recoveries in field samples were 74–93%, 80–97%, 83–105%, and 89–109% for acenaphthene-d10, phenanthrene-d10, chrysene-d12, and perylene-d12 as inferred standards, respectively. The PAH concentrations were not corrected for the recoveries.

Gas/Particle Partitioning Estimation

Octanol–air partition coefficient (K_{OA})-based model has been proved applicable to estimate the gas-particle partitioning of PAHs (Cheruiyot *et al.*, 2015; Cheruiyot *et al.*, 2016; Wang *et al.*, 2018). The temperature–dependent K_{OA} values can be measured directly using the GC retention time method with an equation as Eq. (1) (Harner and Bidleman, 1996):

$$\text{Log } K_{OA} = A + B/(T, K) \quad (1)$$

The regression parameters (A and B) were given by Harner and Bidleman (1998) and Odabasi *et al.* (2006). The difference of K_{OA} values of PAHs among four seasons were calculated by adjusting the equations to the average

Table 1. Parameters of Eq. (1) and octanol-air partition coefficients (K_{OA}) for PAHs at 5°C, 16°C, 14°C and 1.5°C in spring, summer, autumn and winter, respectively.

SN	PAH	A	B	Log K_{OA} (5°C)	Log K_{OA} (16°C)	Log K_{OA} (14°C)	Log K_{OA} (1.5°C)
1	Ace[b]	–2.20	2597	7.14	6.78	6.84	7.22
2	Acel[b]	–1.97	2476	6.93	6.59	6.65	7.01
3	Ant[b]	–3.41	3316	8.51	8.06	8.14	8.62
4	Flu[a]	–7.74	4332	7.58	7.19	7.26	7.67
5	Phe[a]	–5.62	3942	8.47	8.02	8.10	8.58
6	BaA[b]	–5.64	4746	11.4	10.7	10.8	11.5
7	Chr[b]	–5.65	4754	11.5	10.8	10.9	11.6
8	Fla[a]	–5.94	4417	9.70	9.16	9.26	9.83
9	Pyr[a]	–4.56	3985	9.77	9.22	9.32	9.90
10	BaP[b]	–6.50	5382	12.8	12.1	12.2	13.0
11	BbF[b]	–6.40	5285	12.6	11.8	12.0	12.7
12	BkF[b]	–6.42	5301	12.6	11.9	12.1	12.8
13	DahA[b]	–7.17	5887	14.0	13.2	13.3	14.2
14	BghiP[b]	–7.03	5834	13.9	13.1	13.2	14.1
15	IndP[b]	–7.00	5791	13.8	13.0	13.1	14.0

[a] Harner and Bidleman (1998); [b] Odabasi *et al.* (2006).

ambient temperature (pre-monsoon: 5°C, monsoon: 16°C, post-monsoon: 14°C, and winter: 1.5°C) (Table 1). Then the gas-particle partition coefficient (K_P) can be predicted by Eq. (2) if the organic matter fraction *f*om of the aerosols are known and assuming that all of the particle organic matter is available to absorb gas phase compounds.

$$\log K_P = \log K_{OA} + \log f\text{om} - 11.91 \quad (2)$$

In this study, the average organic carbon concentrations were 13.2, 10.2, 30.6, and 35.9 μg m^{-3} for these four seasons in aerosols of sampling site. And organic compounds contributed 18.3%, 16.9%, 25.7%, and 23.9% to total suspended particles in four seasons. Finally, we can estimate the gas phase PAHs using Eq. (3):

$$K_P = (C_p/C_{TSP})/C_g \quad (3)$$

where C_p and C_g are the PAH concentrations in the particulate and gas phases, respectively, and C_{TSP} is the concentration of TSP in the air.

PMF Receptor Model

PMF is a powerful factorization method used to calculate the source profiles and contributions of pollutants in the environment. It has been used extensively for atmospheric source identification (Paatero and Tapper, 1994; Dvorská *et al.*, 2012; Callén *et al.*, 2014). PMF analysis is described in detail in Chen *et al.* (2016). A 62 × 15 (62 samples each containing 15 PAHs) dataset was input into the PMF 5.0 model to conduct source apportionment of atmospheric PAHs in Lhasa. A random seed mode and random starting point were selected. After testing three to six factors, a four-factor solution was adopted. Correlation indices between the estimated and measured concentrations ranged from 0.75 (Ace) to 0.92 (IcdP and BghiP), which suggested that the measured concentrations were fully explained by the four selected factors.

Cancer Risk Assessment

The carcinogenic potency of PAH exposure can be estimated as the sum of each individual BaP equivalent (BaP_{eq}) based on the toxic equivalency factor (TEF) of each individual PAH including both particle and gas phase PAHs (Nisbet and LaGoy, 1992; Petry *et al.*, 1996; US EPA 2010). The TEF data in Nisbet and LaGoy (1999) were used in this study; BaP_{eq} was calculated as follows:

$$\text{Total } BaP_{eq} = \Sigma_i(C_i \times TEF_i) \quad (4)$$

where C_i is the concentration of an individual PAH and TEF_i is its TEF. Inhalation was determined to be the main exposure pathway for PAHs in the air. We applied the following inhalation exposure assessment model recommended by the US EPA to calculate the daily exposure dose (DED) of BaP_{eq}:

$$\text{DED} = \frac{\text{C} \times \text{IR} \times \text{EF} \times \text{ED}}{\text{BW} \times \text{AT}} \times cf \quad (5)$$

where DED is the DED of BaP_{eq} through the inhalation pathway (mg (kg day)$^{-1}$), C is the airborne BaP_{eq} concentration (ng m^{-3}), IR is the air inhalation rate (m^3 day^{-1}), EF is the exposure frequency (day $year^{-1}$), ED is the exposure duration (year), BW is the body weight (kg), AT is the averaging time (day), and *cf* is the conversion factor (in this study, $cf = 10^{-6}$).

The carcinogenic risk (CR) associated with inhalation exposure was calculated using Eq. (6), adapted from the US EPA (1989) and expressed as follows:

$$\text{CR} = \text{DED} \times \text{CSF} \times \left(\frac{\text{BW}}{70}\right)^{1/3} \quad (6)$$

where CR is the probability of developing cancer over a lifetime because of exposure to atmospheric PAHs and

CSF is the cancer slope factor, which quantitatively defines the relationship between carcinogen exposure dose and degree of CR. The CSFs used were derived assuming a body weight of 70 kg, which deviates from the actual conditions of the exposure populations of various age groups. Thus, the CSF values were extrapolated to actual body weights in various age groups by multiplying the conversion factor $(BW/70)^{1/3}$, recommended by the US EPA (2004).

RESULTS AND DISCUSSION

PAH Concentrations and Compositions

During the study period, the particle phase PAH concentrations varied between 9.18 and 211 ng m^{-3} with an average of 45.0 ± 60.4 ng m^{-3} (Table 2). Although the annual average PAH concentration was considerably lower than those reported in numerous areas of northern China such as Shanxi, Shandong, and Beijing (Zhang *et al.*, 2016) and South Asia such as Kathmandu (Chen *et al.*, 2015) and Delhi (Sarkar and Khillare, 2013), it was higher than those observed at background sites in the TP. For example, PAHs in Lulang on the southeastern TP ranged from 0.06 to 2.53, with a mean value of 0.59 ng m^{-3} (Chen *et al.*, 2014). In Zhongba and Nyalam, the mean PAH concentrations were 8.78 and 5.60 ng m^{-3}, respectively (Wang *et al.*, 2014; Chen *et al.*, 2017;). This indicated that although the atmosphere in Lhasa is relatively clean compared to other Asian cities, it is affected by local anthropogenic activities. In addition, the PAH concentration had evidently increased since the two studies conducted in Lhasa in 2006 and 2007 (Table 2), implying that emissions might have increased as a result of urbanization (Gong *et al.*, 2011; Liu *et al.*, 2013).

Evident seasonal variations in the total PAH concentrations were observed, with the maximum and minimum concentrations occurring in winter and summer, respectively (Fig. 2). Based on the Octanol–air partition coefficient (K_{OA}) model, the gas phase PAH concentrations were calculated, which also demonstrated clear seasonal variation with the highest concentrations occurred in summer, decreasing to minimum concentrations in winter (Table 3). Previous studies have reported that seasonal variations of some atmospheric pollutants in Lhasa were mainly influenced by vehicle emissions in summer and biomass burning, power plants, and religious activities during the other seasons (Huang *et al.*, 2010; Gong *et al.*, 2011). During the cold season, biomass or coal combustion for heating increased as the temperature drops (Huang *et al.*, 2010). And the incense burning in the temples for religious activities might be another important emission source of PAHs (Liu *et al.*, 2013). Furthermore, low temperature (–7 to 9°C) strengthens the condensation of gas phase PAHs onto atmospheric particles, leading to higher concentrations of particle phase PAHs in winter (Gong *et al.*, 2011). A greater abundance of PAHs from late autumn to winter implied that PAH contributions from anthropogenic activities increase in the cold season, whereas in summer, although vehicle use and the frequency of tourist activities increase, high rainfall (approximately 70% of the total annual precipitation) washes most suspended particles and particle-

Table 2. Summary of particle-bound PAH concentrations (ng m^{-3}) in Lhasa and other regions.

PAH	Ring	Mean (SD)	Minimum	Maximum	% of ΣPAHs	Reference
Ace	3	0.392 (0.079)	0.297	0.678	0.892	This study
Acel	3	0.405 (0.048)	0.330	0.536	0.922	,,
Ant	3	0.824 (0.298)	0.612	2.074	1.88	,,
Flu	3	0.742 (0.123)	0.545	1.01	1.69	,,
Phe	3	1.94 (2.17)	0.523	10.5	4.41	,,
BaA	4	4.26 (7.71)	0.556	39.9	9.70	,,
Chr	4	5.38 (8.10)	0.956	42.0	12.2	,,
Fla	4	6.71 (10.4)	0.501	55.7	15.3	,,
Pyr	4	6.51 (10.7)	0.865	57.2	14.8	,,
BaP	5	3.93 (5.96)	0.654	28.1	8.94	,,
BbF	5	5.59 (7.72)	0.887	21.6	9.48	,,
BkF	5	2.01 (3.72)	0.529	18.9	7.81	,,
DahA	5	0.849 (0.402)	0.582	2.29	1.93	,,
BghiP	6	2.30 (2.52)	0.710	12.1	5.24	,,
IndP	6	2.09 (2.64)	0.565	12.0	4.77	,,
Total PAHs		43.9 (54.6)	9.18	211	100	,,
Beijing[a]		148 (28)		-		Zhang *et al.*, 2016
Delhi[b]		105	11.0	512		Sarkar and Khillare, 2013
Kathmandu[c]		155 (130)	18.1	453		Chen *et al.*, 2015
Zhongba[c]		8.78 (4.50)	3.41	20.9		Chen *et al.*, 2017
Nyalam[c]		5.57 (3.36)	3.62	16.9		Chen *et al.*, 2017
Lulang[d]		0.59 (0.52)	0.06	2.53		Chen *et al.*, 2014
Lhasa[e]		20 (15)	4.4	60		Liu *et al.*, 2013
Lhasa[f]		35.7 (15.9)	11.4	72.5		Gong *et al.*, 2011

[a] 16 PAHs of TSP samples; [b] 16 PAHs of PM_{10} samples; [c] 15 PAHs of TSP samples; [d] 17 PAHs of TSP samples; [e] 15 PAHs of TSP samples; [f] 22 PAHs of TSP samples.

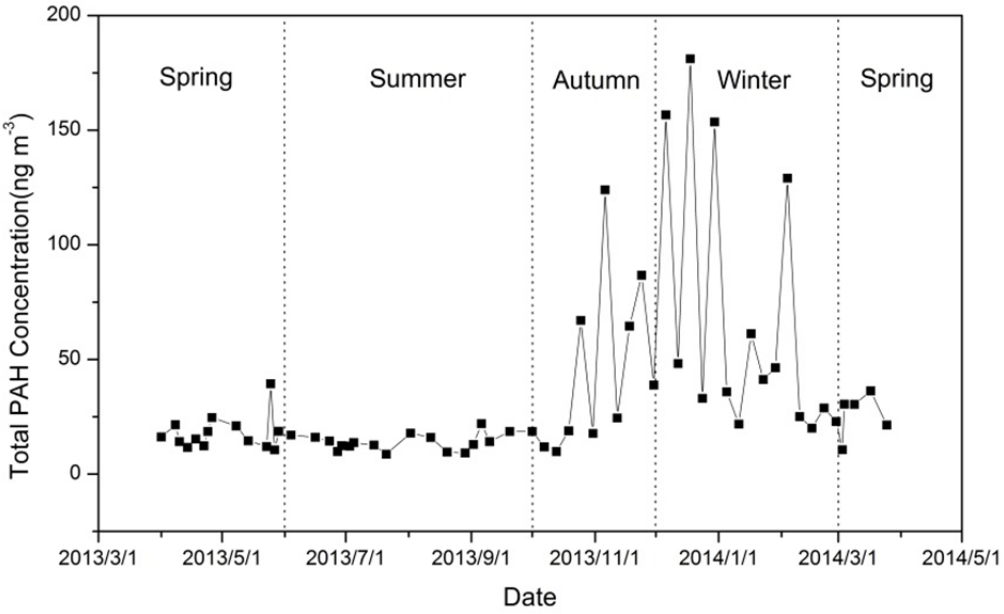

Fig. 2. Seasonal variations of PAH concentrations in Lhasa.

Table 3. Calculated gas phase PAH concentrations in four seasons of Lhasa.

SN	PAH	Spring	Summer	Autumn	Winter
1	Ace	506.2597	1528.076	448.5648	183.0286
2	Acel	893.5951	2440.036	732.5843	289.8921
3	Ant	80.33509	290.3747	82.25962	28.92283
4	Flu	497.3334	1239.61	681.354	562.8298
5	Phe	93.16859	335.6044	101.9659	37.49022
6	BaA	0.507878	0.912246	0.87494	0.523964
7	Chr	0.423029	0.867332	0.866197	0.493445
8	Fla	11.77585	22.81812	28.92497	19.83927
9	Pyr	17.74505	37.10413	31.53879	19.42907
10	BaP	0.013702	0.063772	0.064483	0.013267
11	BbF	0.013721	0.064625	0	0.010735
12	BkF	0.014141	0.047081	0.046888	0.017806
13	DahA	0.000416	0.002468	0.002228	0.000309
14	BghiP	0.000295	0.002407	0.000836	0.000104
15	IndP	0.000773	0.005072	0.00348	0.000478
	Total	2101.187	5895.588	2109.051	1142.492

bound pollutants out of the atmosphere (Cong *et al.*, 2011; Wan *et al.*, 2016). In addition, the high summer temperature (9–22°C) enhances the evaporation of particle phase to gas phase PAHs, which leads to lower PAH concentrations in summer (Tham *et al.*, 2008; Liu *et al.*, 2017b); for example, the contribution of PAHs with low molecular weights (e.g., Ace, Acel, Ant, Flu, and Phe) was twice as high in winter as in summer, indicating that temperature is a crucial factor possibly resulting in seasonal variations between PAH concentrations.

According to the number of aromatic rings, the aforementioned 15 PAHs were classified into four groups: three-ring (Acel, Ace, Flu, Phe, and Ant), four-ring (Fla, Pry, BaA, and Chr), five-ring (BbF, BkF, BaP, and DahA), and six-ring (IndP and BghiP) PAHs (Kaur *et al.*, 2013). The seasonal composition patterns of the particle phase 15 PAHs over four seasons are shown in Fig. 3; four- and five-ring PAHs contributed the most, followed by six- and three-ring PAHs. Correspondingly, gas phase PAHs showed different composition patterns with three-ring compounds especially Aec, Acel, and Flu contributed most to the total particles (Table 3). However, the profiles of particle phase PAHs in Lhasa varied across all four seasons; for example, the contributions of four-ring PAHs were highest in winter at 56.5%, which decreased to 31.5% in summer. By contrast, the contributions of five- and six-ring PAHs exhibited the opposing trend. Previous studies have reported that coal combustion and biomass burning release an abundance of four-ring PAHs, whereas five- and six-ring PAHs mainly originate from high-temperature combustion processes such as vehicle exhaust (Dachs *et al.*, 2000; Moon *et al.*, 2008). The variations in PAH compositions evidently reflect

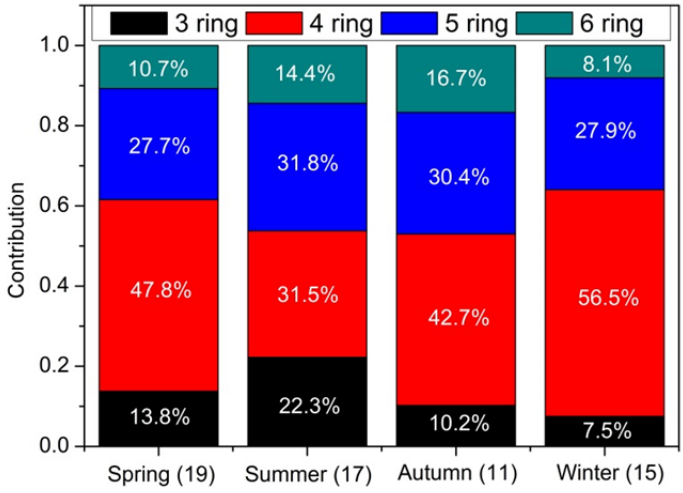

Fig. 3. Seasonal variations of PAH compositions (three-, four-, five-, and six-ring PAHs) in Lhasa, number in bracket are sample sizes.

the aforementioned changes in source contributions during the sampling period (Huang *et al.*, 2010; Gong *et al.*, 2011). Meanwhile, the partitioning of PAHs between the particle- and gas phase is temperature sensitive and consequently four-ring compounds making an apparently greater contribution in winter as opposed to summer.

PAH Sources Assessed By Diagnostic Ratios

Diagnostic ratios are used frequently to identify PAH origins (Yunker *et al.*, 2002; Rajput *et al.*, 2014). In this study, IndP/(IndP + BghiP) and Fla/(Fla + Pyr) ratios were used simultaneously to cross-check the results and reduce uncertainty. The IndP/(IndP + BghiP) ratios were below 0.5 in all seasons, implying a strong contribution from petroleum combustion (Table 4). The mean Fla/(Fla + Pyr) ratios were 0.54 ± 0.03, 0.48 ± 0.02, 0.49 ± 0.02, and 0.52 ± 0.03 in spring, summer, autumn, and winter, respectively, with lower values in summer and autumn, thereby reflecting the impact of vehicles as PAH sources (Table 4). The tourist activities mainly happen from May to October especially in summer. And vehicle emission is higher during this period than the cold season. Higher values were observed in winter and spring, implying that the biomass contribution increased in these seasons because of low temperatures. Biomass energy consumption was considered as the largest parts (about 40%) of total energy consumption, compared to coal and liquid fossil fuel, 5% and 16%, respectively (Hua, 2009). These results are consistent with those of the PMF model in Subsection 3.3.

Source Apportionment of All PAHs Determined Using PMF

Fig. 4 shows the four source contributions of all samples and PMF factors of all profiles and contributions. Each column corresponds to the concentration profile of one PAH. The first factor accounted for 9.30% of all PAHs. The profile contains more volatile PAHs, which are similar to those reported as air–ground and air–soil emissions (Nelson *et al.*, 1998; Cheng *et al.*, 2012). Accordingly, the first factor was classified as air–surface exchange. The second factor accounted for 14.3% of all PAHs and showed high loadings of Fla and Pyr, which are typical markers of coal combustion (Huang *et al.*, 2010; Qin *et al.*, 2014). Thus, this factor was classified as coal emission. The third factor accounted for 48.4% of all PAHs and had high loadings of four-ring PAHs such as Fla, Pyr, and Chr and moderate contributions from BaA, Bbf, Bkf, and Bap. This type of profile is mainly the result of biomass burning (Lin *et al.*, 2011; Wang *et al.*, 2015). In Lhasa, biomass varieties such as wood and yak dung are burned year-round for heating and cooking, especially in winter (Huang *et al.*, 2010). Thus, this factor was assigned as biomass burning. The fourth factor

Table 4. Diagnostic ratios of PAHs in Lhasa aerosols and their source profiles. Numbers in brackets represent standard deviations.

	Spring	Summer	Autumn	Winter	Source profiles	Reference
IndP/(IndP + BghiP)	0.44 (0.03)	0.42 (0.02)	0.47 (0.03)	0.47 (0.03)	< 0.2 Petrogenic 0.2–0.5 Petroleum combustion > 0.5 Coal and biomass	(Grimmer *et al.*, 1983; Yunker *et al.*, 2002)
Fla/(Fla + Pyr)	0.54 (0.03)	0.48 (0.02)	0.49 (0.02)	0.52 (0.03)	< 0.4 Petrogenic 0.4–0.5 Petroleum combustion > 0.5 Coal and biomass	(Sicre *et al.*, 1987; Tsapakis and Stephanou, 2003; Tang *et al.*, 2005; Bari *et al.*, 2011)

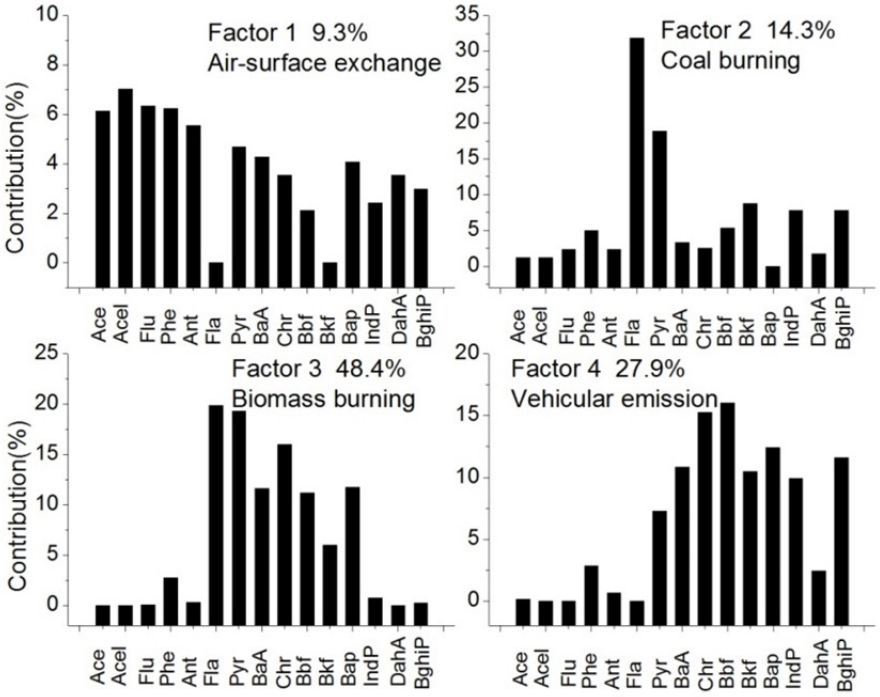

Fig. 4. PMF 5.0-generated factor profiles and their contributions to the 15 examined PAHs.

contributed 27.9% of all PAHs. High loadings of five- and six-ring PAHs were observed. IndP and BghiP are typical markers of traffic emissions (Simcik *et al.*, 1999) and IndP is associated with diesel emissions (Li and Kamens, 1993). A similar profile was observed in aerosols at a site downwind of East Asia (Wang *et al.*, 2014). As a famous tourist city, Lhasa has undergone a rapid increase in vehicle use in recent years, especially in summer and autumn. Therefore, this factor was deemed to be caused by vehicle emissions.

In summary, the main source of atmospheric PAHs in Lhasa is biomass combustion, followed by vehicle emissions, coal combustion, and air–surface exchange. However, notably, determining precise source contributions based on the PMF model and diagnostic ratios only is difficult because of high uncertainty. In addition, the PAH source profiles for coal combustion and residential biomass combustion are usually similar, thereby engendering difficulties in separating these two factors. Thus, further research integrating other methods or evidence is required.

Health Risk Values

The BaP_{eq} values for particle phase PAHs during the sampling period varied from 1.48 to 24.5 ng m^{-3} with an average of 6.27 ± 8.55 ng m^{-3}. For gas phase PAHs, the BaP_{eq} values were 4.28, 11.6, 6.23, and 3.64 ng m^{-3} for spring, summer, autumn, and winter, respectively with an similar average value (6.43 ± 4.15 ng m^{-3}) with particle phase PAHs. The most recent ambient air quality standard for China (GB3095-2012) showed an improvement in the limited value of atmospheric BaP from 10 to 1 ng m^{-3}. All BaP_{eq} concentrations calculated in Lhasa were higher than the limit value, which indicates the potential for adverse health effects caused by atmospheric PAHs in this region.

People of three age groups (children, teenagers, and adults) were examined to effectively estimate the exposure levels of BaP_{eq} in various age ranges. Table 5 shows the parameters of these three age groups used in the exposure assessment. Based on the data, the DEDs and CR of BaP_{eq} in Lhasa were characterized for all three age groups. The CRs of particle phase PAHs were estimated as 9.20×10^{-7}, 7.20×10^{-7}, and 2.84×10^{-6} for children, teens, and adults, respectively. While for gas phase PAHs, the CRs were similar with particle phase PAHs for three groups, with values as 9.43×10^{-7}, 7.38×10^{-7}, and 2.91×10^{-6}. The CR values of total (gas and particle phase) PAHs were 1.86×10^{-6}, 1.46×10^{-6}, and 5.76×10^{-6}, respectively, which were one time higher than those of particle phase PAHs. PAHs are present in the atmosphere in both particle and gas phases. In this study, the calculated gas phase PAH concentrations were much higher than those of particle phase. And CR values doubled after adding gas phase PAHs. Therefore, additional detailed surveys of gas phase PAHs should be considered

Table 5. Values and probability distributions of parameters used in the exposure assessment.

units	Children	Teens	Adults
Age (year)	0–10	11–20	21–70
IR[a] (m^3 day^{-1})	8.79	13.61	12.34
EF (day $year^{-1}$)	365	365	365
ED (year)	0–10	0–10	0–50
BW[b] (kg)	16.66	46.35	57.04
AT[a] (day)	25550	25550	25550
CFS[c] (mg (kg day))$^{-1}$	3.14	3.14	3.14

[a] cited from the US EPA; [b] citied from statistical data from China; [c] cited from Chen and Liao (2006).

in further study. Most regulatory programs employ a limiting CR value of 1.00E–05 (De Miguel *et al.*, 2007). The lifetime CR (LCR) in Lhasa was determined by calculating the CR values of two types of PAHs for all three age groups. The results showed that the LCR (9.08×10^{-6}) was lower than the acceptable target risk value, indicating that atmospheric PAHs in Lhasa pose no or little potential CR to locals.

CONCLUSION

The PAH concentrations in Lhasa were higher than those at other remote sites in the TP, indicating that the atmospheric environment in Lhasa has been influenced by local anthropogenic activities. Clear seasonal variations of PAH concentrations were observed, with maximum and minimum values occurring in winter and summer, respectively. The concentrations of gas phase PAHs were much higher than those of particle phase PAHs, and the two phases exhibited opposite seasonal trends. Particle phase PAH profiles, especially those of four-ring compounds, changed significantly between winter and summer, thereby reflecting the variation in emission sources across different seasons. However, three-ring species, especially Ace, Acel, and Flu, contributed the most to gas phase PAHs. The particle phase PAH sources were quantified using the PMF model, and the results revealed that atmospheric PAHs in Lhasa originated mainly in the combustion of biomass fuels (48.4%) and vehicle emissions (27.9%), which was supported by the diagnostic molecular ratios. The average BaP_{eq} of the PAHs was higher than the new limit in China, thereby indicating potential adverse health effects on local inhabitants. However, a probabilistic health risk assessment showed that atmospheric PAHs in Lhasa posed little or no CR.

ACKNOWLEDGEMENTS

This study is supported by the National Natural Science Foundation of China (41705132, 41630754, 41675130), State Key Laboratory of Cryosphere Science (SKLCS-OP-2018-01) and Chinese Academy of Sciences (QYZDJ-SSW-DQC039). The authors acknowledge Xi Luo for collecting the samples. The manuscript was edited by Wallace Academic Editing.

REFERENCES

Bari, M., Baumbach, G., Brodbeck, J., Struschka, M., Kuch, B., Dreher, W. and Scheffknecht, G. (2011). Characterisation of particulates and carcinogenic polycyclic aromatic hydrocarbons in wintertime wood-fired heating in residential areas. *Atmos. Environ.* 45: 7627–7634.

Bhargava, A., Khanna, R., Bhargava, S. and Kumar, S. (2004). Exposure risk to carcinogenic PAHs in indoor-air during biomass combustion whilst cooking in rural India. *Atmos. Environ.* 38: 4761–4767.

Callén, M., Iturmendi, M. and López, J. (2014). Source apportionment of atmospheric $PM_{2.5}$-bound polycyclic aromatic hydrocarbons by a PMF receptor model. Assessment of potential risk for human health. *Environ. Pollut.* 195: 167–177.

Chen, P., Kang, S., Bai, J., Sillanpää, M. and Li, C. (2015a). Yak dung combustion aerosols in the Tibetan Plateau: Chemical characteristics and influence on the local atmospheric environment. *Atmos. Res.* 156: 58–66.

Chen, P., Kang, S., Li, C., Rupakheti, M., Yan, F., Li, Q., Ji, Z., Zhang, Q., Luo, W. and Sillanpää, M. (2015b). Characteristics and sources of polycyclic aromatic hydrocarbons in atmospheric aerosols in the Kathmandu Valley, Nepal. *Sci. Total Environ.* 538: 86–92.

Chen, P., Li, C., Kang, S., Rupakheti, M., Panday, A., Yan, F., Li, Q., Zhang, Q., Guo, J., Ji, Z., Rupakheti, D. and Luo, W. (2017). Characteristics of particulate-phase polycyclic aromatic hydrocarbons (PAHs) in the atmosphere over the central Himalayas. *Aerosol Air Qual. Res.* 17: 2942–2954.

Chen, S. and Liao, C. (2006). Health risk assessment on human exposed to environmental polycyclic aromatic hydrocarbons pollution sources. *Sci. Total Environ.* 366: 112–123.

Chen, Y., Cao, J., Zhao, J., Xu, H., Arimoto, R., Wang, G., Han, Y., Shen, Z. and Li, G. (2014). *n*-Alkanes and polycyclic aromatic hydrocarbons in total suspended particulates from the southeastren Tibetan Plateau: Concentrations, seasonal variations, and sources. *Sci. Total Environ*. 470: 9–18.

Cheng, H., Deng, Z., Chakraborty, P., Liu, D., Zhang, R., Xu, Y., Luo, C., Zhang, G. and Li, J. (2013). A comparison study of atmospheric polycyclic aromatic hydrocarbons in three Indian cities using PUF disk passive air samples. *Atmos. Environ.* 73: 16–21.

Cheruiyot, N.K., Lee, W.J., Mwangi, J.K., Wang, L.C., Lin, N.H., Lin, Y.C., Cao, J., Zhang, R. and Chang-Chien, G.P. (2015). An overview: Polycyclic aromatic hydrocarbon emissions from the stationary and mobile sources and in the ambient air. *Aerosol Air Qual. Res.* 15: 2730–2762.

Cheruiyot, N.K., Lee, W.J., Yan, P., Mwangi, J.K., Wang, L.C., Gao, X., Lin, N.H. and Chang-Chien, G.P. (2016). An overview of PCDD/F inventories and emission factors from stationary and mobile sources: What we know and what is missing. *Aerosol Air Qual. Res.* 16: 2965–2988.

Cong, Z., Kang, S., Luo, C., Li, Q., Huang, J., Gao, S. and Li, X. (2011). Trace elements and lead isotopic composition of PM_{10} in Lhasa, Tibet. *Atmos. Environ.* 45: 6210–6215.

Cong, Z., Kang, S., Kawamura, K., Liu, B., Wan, X., Wang, Z., Gao, S. and Fu, P. (2015). Carbonaceous aerosols on the south edge of the Tibetan Plateau: concentrations, seasonality and sources. *Atmos. Chem. Phys.* 15: 1573–1584.

Dachs, J. and Eisenreich, S. (2000). Adsorption onto aerosol soot carbon dominates gas-particle partitioning of polycyclic aromatic hydrocarbons. *Environ. Sci. Technol.* 34: 3690–3697.

Dvorská, A., Komprdová, K., Lammel, G., Klánová, J. and Helena, P. (2012). Polycyclic aromatic hydrocarbons in background air in central Europe-seasonal levels and limitations for source apportionment. *Atmos. Environ.* 46: 147–154.

Gong, P., Wang, X. and Yao, T. (2011). Ambient distribution of particulate- and gas-phase n-alkanes and polycyclic aromatic hydrocarbons in the Tibetan Plateau. *Environ. Earth Sci.* 64: 1703–1711.

Grimmer, G., Jacob, J. and Naujack, K. (1983). Profile of the polycyclic aromatic compounds from crude oils. *Fresenius Z. Anal. Chem.* 314: 29–36.

Halsall, C., Sweetman, A., Barrie, L. and Jones, K. (2001). Modelling the behaviour of PAHs during atmospheric transport form the UK to the Arctic. *Atmos. Environ.* 35: 255–267.

Harner, T. and Bidleman, T. (1996). Measurements of octanol-air partition coefficients for polychlorinated biphenyls. *J. Chem. Eng. Data*. 41: 895–899.

Harner, T. and Bidleman, T. (1998). Octanol-air partition coefficient for describing particle/gas partitioning of aromatic compounds in urban air. *Environ. Sci. Technol.* 32: 1497–1502.

Hua, H. (2009). The research on the usage of energy in Lhasa area. *Energy Res. Util*. 30–32 (in Chinese).

Huang, H., Blanchard, P., Halsall, C., Bidleman, T., Stem, G., Fellin, P., Muir, D., Barrie, L., Jantunen, L., Helm, P., Ma, J. and Konoplev, A. (2005). Temporal and spatial variabilities of atmospehric polychlorinated biphenyls (PCBs), organochlorine (OC) pesticides and polycyclic aromatic hydrocarbons (PAHs) in the Canadian Arctic: Results from a decade of monitoring. *Sci. Total Environ.* 342: 119–144.

Huang, J., Kang, S., Shen, C., Cong, Z., Liu, K., Wang, W. and Liu, L. (2010). Seasonal variations and sources of ambient fossil and biogenic-derived carbonaceous aerosols based on ^{14}C measurements in Lhasa, Tibet. *Atmos. Res.* 96: 553–559.

Huang, J., Kang, S., Wang, S., Wang, L., Zhang, Q., Guo, J., Wang, K., Zhang, G. and Tripathee, L. (2013). Wet deposition of mercury at Lhasa, the capital city of Tibet. *Sci. Total Environ.* 447: 123–132.

Kaur, S., Senthilkumar, K., Verma, V., Kumar, B., Kumar, S., Katnoria, J. and Sharma, C. (2013). Preliminary analysis of polycyclic aromatic hydrocarbons in air particles (PM_{10}) in Amritsar, India: sources, apportionment, and possible risk implications to humans. *Arch. Environ. Contam. Toxicol.* 65: 382–395.

Lai, Y., Tsai, C., Liang, Y. and Chien, G. (2017). Distribution and sources of atmospheric polycyclic aromatic hydrocarbons at an industrial region in Kaohsiung, Taiwan. *Aerosol Air Qual. Res.* 17: 776–787.

Li, C. and Kamens, R. (1993). The use of polycyclic aromatic hydrocarbons as source signatures in receptor modelling. *Atmos. Environ.* 27: 523–532.

Li, C., Kang, S., Chen, P., Zhang, Q. and Fang, G. (2012). Characterizations of particle-bound trace metals and polycyclic aromatic hydrocarbons (PAHs) within Tibetan tents of south Tibetan Plateau, China. *Environ. Sci. Pollut. Res.* 19: 1620–1628.

Li, C., Bosch, C., Kang, S., Andersson, A., Chen, P., Zhang, Q., Cong, Z., Chen, B., Qin, D. and Gustafsson, Ö. (2016a). Sources of black carbon to the Himalayan-Tibetan Plateau glaciers. *Nat. Commun.* 7: 12574.

Li, C., Chen, P., Kang, S., Yan, F., Hu, Z., Qu, B. and Sillanpää, M. (2016b). Concentrations and light absorption characteristics of carbonaceous aerosol in $PM_{2.5}$ and PM_{10} of Lhasa city, the Tibetan Plateau. *Atmos. Environ.* 127: 340–346.

Li, J., Lin, T., Qi, S., Zhang, G., Liu, X. and Li, K. (2008). Evidence of local emission of organochlorine pesticides in the Tibetan plateau. *Atmos. Environ.* 42: 7397–7404.

Li, Q. and Wang, C. (2014). Research on urbanization in Tibet and its environmental impact. *Chinese Soft Sci. Mag*. 12: 70–78 (in Chinese).

Lin, T., Hu, L., Guo, Z., Qin, Y., Yang, Z., Zhang, G. and Zheng, M. (2011). Sources of polycyclic aromatic hydrocarbons to sediments of the Bohai and Yellow Seas in East Asia. *J. Geophy. Res.* 116: D23305.

Liu, J., Li, J., Lin, T., Liu, D., Xu, Y., Chaemfa, C., Qi, S., Liu, F. and Zhang, G. (2013). Diurnal and nocturnal variations of PAHs in the Lhasa atmosphere, Tibetan Plateau: Implication for local sources and the impact of atmospheric degradation processing. *Atmos. Res.* 124: 34–43.

Liu, J., Wang, Y., Li, P., Shou, Y., Li, T., Yang, M., Wang, L., Yue, J., Yi, X. and Guo, L. (2017a). Polycyclic aromatic hydrocarbons (PAHs) at high mountain site in north China: Concentration, source and health risk assessment. *Aerosol Air Qual. Res.* 17: 2867–2877.

Liu, X., Li, C., Tu, H., Wu, Y., Ying, C., Huang, Q., Wu, S., Xie, Q., Yuan, Z. and Lu, Y. (2017b). Analysis of the effect of meteorological factors on $PM_{2.5}$-associated PAHs during autumn-winter in urban Nanchang. *Aerosol Air Qual. Res.* 17: 3222–3229.

Lüthi, Z., Škerlak, B., Kim, S., Lauer, A., Mues, A., Rupakheti, M. and Kang, S. (2015). Atmospheric brown clouds reach the Tibetan Plateau by crossing the Himalayas. *Atmos. Chem. Phys.* 15: 1–15.

Moon, K., Han, J., Ghim, Y. and Kim, Y. (2008). Source apportionment of fine carbonaceous particles by positive matrix factorization at Gosan backgroud site in East Asia. *Environ. Int.* 34: 654–664.

Nelson, E., McConnell, L. and Baker, J. (1998). Diffusive exchange of gaseous polycyclic aromatic hydrocarbons and polychlorinated biphenyls across the air-water interface of the Chesapeake Bay. *Environ. Sci. Technol.* 32: 912–919.

Nisbet, I. and LaGoy, P. (1992). Toxic equivalency factors (TEFs) for polycyclic aromatic hydrocarbons (PAHs). *Regul. Toxicol. Pharm.* 16: 290–300.

Odabasi, M., Cetin, E. and Sofuoglu, A. (2006). Determination of octanol-air partition coefficients and supercooled liquid vapor pressures of PAHs as a function of temperature: Application to gas-particle partitioning in an urban atmosphere. *Atmos. Environ.* 40: 6615–6625.

Paatero, P. and Tapper, U. (1994). Positive matrix factorization: A non-negative factor model with optimal utilization of error estimates of dara values. *Environmetrics* 5: 111–126.

Petry, T., Schmid, P. and Schlatter, C. (1996). The use of toxic equivalency factors in assessing occupational and environmental health risk associated with exposure to

airborne mixtures of polycyclic aromatic hydrocarbons (PAHs). *Chemosphere* 32: 639–648.

Qin, L., Han, J., He, X. and Lu, Q. (2014). The emission characteristic of PAHs during coal combustion in a fluidized bed combustor. *Energy Sources Part A* 36: 212–221.

Rajput, P., Sarin, M., Sharma, D. and Singh, D. (2014). Atmospheric polycyclic aromatic hydrocarbons and isomer ratios as tracers of biomass burning emissions in Northern India. *Environ. Sci. Pollut. Res.* 21: 5724–5729.

Ran, L., Lin, W.L., Deji, Y.Z., La, B., Tsering, P.., Xu, B.Q. and Wang, W. (2014). Source gas pollutants in Lhasa, a highland city of Tibet-current levels and pollution implications. *Atmos. Chem. Phys.* 14: 10721–10730.

Ravindra, K., Sokhi, R. and Van Gridken, R. (2008). Atmospheric polycyclic aromatic hydrocarbons: Source attribution, emission factors and regulation. *Atmos. Environ.* 42: 2895–2921.

Saha, M., Maharana, D., Kurumisawa, R., Takada, H., Yeo, B., Rodrigues, A., Bhattacharya, B., Kumata, H., Okuda, T., He, K., Ma, Y., Nakajima, F., Zakaria, M., Giang, D. and Viet, P. (2017). Seasonal trends of atmospheric PAHs in five Asian megacities and source detection using suitable biomarkers. *Aerosol Air Qual. Res.* 17: 2247–2262.

Sarkar, S. and Khillare, P. (2013). Profile of PAHs in the inhalable particulate fraction: source apportionment and associated health risks in a tropical megacity. *Environ. Monit. Assess.* 185: 1199–1213.

Sicre, M., Marty, J., Saliot, A., Aparicio, X., Grimalt, J. and Albaiges, J. (1987). Aliphatic and aromatic hydrocarbons in different sized aerosols over the Mediterranean Sea: occurrence and origin. *Atmos. Environ.* 21: 2247–2259.

Tang, N., Hattori, T., Taga, R., Igarashi, K., Yang, X., Tamura, K., Kakimoto, H., Mishukov, V., Toriba, A. and Kizu, R. (2005). Polycyclic aromatic hydrocarbons and nitropolycyclic aromatic hydrocarbons in urban air particulates and their relationship to emission sources in the Pan–Japan Sea countries. *Atmos. Environ.* 39: 5817–5826.

Tao, S., Wang, W., Liu, W., Zuo, Q., Wang, X., Wang, R., Wang, B., Shen, G., Yang, Y. and He, J. (2010). Polycyclic aromatic hydrocarbons and organochlorine pesticides in surface soils from the Qinghai-Tibetan plateau. *J. Environ. Monit.* 13: 175–181.

Tham, Y., Takeda, K. and Sakugawa, H. (2008). Polycyclic aromatic hydrocarbons (PAHs) associated with atmospheric particles in Higashi Hiroshima, Japan: Influence of meteorological conditions and seasonal variations. *Atmos. Res.* 88: 224–233.

Tsapakis, M. and Stephanou, E. (2003). Collection of gas and particle semi-volatile organic compounds: Use of an oxidant denuder to minimize polycyclic aromatic hydrocarbons degradation during high-volume air sampling. *Atmos. Environ.* 37: 4935–4944.

US EPA (1989). Risk assessment guidance for superfund volume I: Human health evaluation manual (Part A). EPA/540/1-89/002. http://www.epa.gov/oswer/riskassessment/ragsa/pdf/rags-vol1-pta_complete.pdf

US EPA (2004). Risk assessment guidance for superfund volume I: Human health evaluation manual (Part E, supplemental guidance for dermal risk assessment). EPA/540/R/99/005. http://www.epa.gov/superfund/programs/risk/ragse/index.htm

Wan, X., Kang, S., Xin, J., Liu, B., Wen, T., Wang, P., Wang, Y. and Cong, Z. (2016). Chemical composition of size-segregated aerosols in Lhasa city, Tibetan Plateau. *Atmos. Res.* 174: 142–150.

Wang, C., Wang, X., Gong, P. and Yao, T. (2014). Polycyclic aromatic hydrocarbons in surface soil across the Tibetan Plateau: Spatial distribution, source and airesoil exchange. *Environ. Pollut.* 184: 138–144.

Wang, F., Lin, T., Feng, J., Fu, H. and Guo, Z. (2015). Source apportionment of polycyclic aromatic hydrocarbons in $PM_{2.5}$ using positive matrix factorization modeling in Shanghai, China. *Environ. Sci. Processes Impacts* 17: 197–205.

Wang, W., Cui, K., Zhao, R., Zhu, J., Huang, Q. and Lee, W.J. (2018). Sensitivity analysis of $PM_{2.5}$-bound total PCDD/Fs-TEQ content: In the case of Wuhu City, China. *Aerosol Air Qual. Res.* 18: 407–420.

Yang, T., Hsu, C., Chen, Y., Young, L., Huang, C. and Ku, C. (2017). Chatacterisitics, sources, and health risks of atmospheric $PM_{2.5}$-bound polycyclic aromatic hydrocarbons in Hsinchu, Taiwan. *Aerosol Air Qual. Res.* 17: 563–573.

Yunker, M., Macdonald, R., Vingarzan, R., Mitchell, R., Goyette, D. and Sylvestre, S. (2002). PAHs in the Fraser River basin: A critical appraisal of PAH ratios as indicators of PAH source and composition. *Org. Geochem.* 33: 489–515.

Zhang, Y. and Tao, S. (2009). Global atmospheric emission inventory of polycyclic aromatic hydrocarbons (PAHs) for 2004. *Atmos. Environ.* 43: 812–819.

Zhang, Y., Lin, Y., Cai, J., Liu, Y., Hong, L., Qin, M., Zhao, Y., Ma, J., Wang, X., Zhu, T., Qiu, X. and Zheng, M. (2016). Atmospheric PAHs in North China: Spatial distribution and sources. *Sci. Total Environ.* 565: 994–1000.

Received for review, January 13, 2018
Revised, March 24, 2018
Accepted, March 25, 2018